

Modulation of South Indian Ocean Tropical Cyclones by the Madden–Julian Oscillation and Convectively Coupled Equatorial Waves

MILLOUD BESSAFI

Laboratoire de Génie Industriel, Université de La Réunion, Réunion Island, France

MATTHEW C. WHEELER

Bureau of Meteorology Research Centre, Melbourne, Australia

(Manuscript received 19 April 2005, in final form 14 June 2005)

ABSTRACT

The subseasonal modulation of tropical cyclone (TC) genesis by large-scale atmospheric wave modes is studied using data from the south Indian Ocean region. The modes considered are the Madden–Julian oscillation (MJO), and the convectively coupled equatorial Rossby (ER), Kelvin, and mixed Rossby–gravity (MRG) waves. Analysis of all TCs west of 100°E reveals a large and statistically significant modulation by the MJO and ER waves, a small yet significant modulation by Kelvin waves, and a statistically insignificant modulation by MRG waves. Attribution of the observed TC modulation was made through examination of the wave-induced perturbations to the dynamical fields of low-level vorticity, vertical shear, and deep convection. Possible thermodynamic influences on TC genesis were neglected. Different combinations of the three dynamical fields were necessary for successful attribution for each of the large-scale wave modes. For example, for the MJO, the modulation was best attributable to its perturbations to both the vorticity and shear fields, while for the ER wave, it was its perturbations to the convection and vorticity fields that appeared to best be able to explain the modulation. It appears that there is no single factor that can be used for the attribution of all subseasonal TC variability. Finally, it is shown that the modulation of TCs by at least the MJO and ER waves is large enough to warrant further investigation for prediction on the weekly time scale.

1. Introduction

This study is aimed at documenting and understanding aspects of subseasonal variability of tropical cyclone (TC) genesis over the south Indian Ocean. We focus on the modulation of TC genesis by the various large-scale waves, or modes that exist coupled with convection in the tropical atmosphere. The modes considered are the Madden–Julian oscillation (MJO; e.g., Madden and Julian 1994) and the convectively coupled equatorial Rossby (ER), Kelvin, and mixed Rossby–gravity (MRG) waves (e.g., Wheeler et al. 2000).

Previous published work on subseasonal variability of TC genesis extends as far back as Gray (1979), who found that the global count of TC formations have a

tendency to be clustered into 2–3-week active periods, separated by 2–3-week periods of relatively fewer formations. This periodicity suggested to researchers that there was an important role for planetary-scale intraseasonal variability, like the MJO, for TC development. Subsequently, Nakazawa (1986), using data from the year 1979, found a modulation of regional TC activity specifically at the 30- to 60-day time scale ascribed to the MJO. TCs were found to preferentially occur at times and locations where the 30–60-day fluctuations in convection were in their enhanced (active) phase. Building on this, Liebmann et al. (1994), using many years of TC reports between 60°E and 180°, found an approximately 2:1 modulation of the occurrence of TCs using a 35- to 95-day filtered definition of the MJO. In a more focused study, Maloney and Hartmann (2000b) looked at the modulation of TCs in the eastern North Pacific using 20- to 80-day filtered 850-hPa zonal wind to define the MJO. They found that hurricane-strength systems were 4 times more likely during times of a west-

Corresponding author address: Prof. Miloud Bessafi, University of La Réunion, 15, Avenue René Cassin, B.P. 7151, 97715 Saint-Denis Cedex 9, Réunion Island, France.
E-mail: miloud.bessafi@univ-reunion.fr

erly wind anomaly than an easterly. This result was attributed to the MJO influence on two large-scale dynamical parameters thought to be important for TC development: low-level vorticity and vertical wind shear. Indeed, there has been a long line of work documenting the importance of certain large-scale dynamical and thermodynamic conditions for TC development (e.g., Gray 1968, 1979; McBride and Zehr 1981; Frank 1987), and it is presumable that the MJO is able to perturb such “climatologically favorable conditions” to an extent that TC genesis is affected.

Subsequent to the initial MJO–TC work, the modulation of TCs by the MJO has also received focused study in the region of the Gulf of Mexico (Maloney and Hartmann 2000a), the western North Pacific (Sobel and Maloney 2000), around Australia (Hall et al. 2001), and in a case study of the eastern Pacific (Molinari et al. 1997; Molinari and Vollaro 2000). Using 20 yr (1976–96) of best-track TC data, Hall et al. (2001) determined that the MJO strongly modulates the pattern of TC genesis in the Southern Hemisphere between the longitudes of 80° and 170°E, in accord with the large-scale variations in 850-hPa relative vorticity. Given the extended-range predictability of the MJO (e.g., Waliser et al. 2003; Wheeler and Weickmann 2001; and references therein), the obvious benefits of finding relationships between the MJO and TCs have been expounded in these studies. However, no study on subseasonal variability of TCs has been undertaken specifically for the south Indian Ocean region.

Besides the MJO, other defined modes of subseasonal tropical variability, which presumably have the possibility for modulating TCs, also exist. The ER wave, Kelvin wave, and MRG wave are the lowest frequency of the shallow-water-like equatorial waves that have been observed coupled with large-scale convection (Wheeler and Kiladis 1999). Although they each account for less variability than the MJO, they still significantly influence the large-scale atmospheric fields (Wheeler et al. 2000), and at times have amplitudes large enough to be delineated in unfiltered data (e.g., Straub and Kiladis 2002; Wheeler and McBride 2005), and thus may also be implicated in TC development. Indeed, evidence has been presented in the literature suggesting TCs respond to arbitrarily chosen bands of large-scale subseasonal variability, and not just the MJO (Liebmann et al. 1994). An example is in the work of Hartmann et al. (1992), who found a 20–25-day oscillation of TCs in the western North Pacific. Except for the work of Dickinson and Molinari (2002), however, who found an association between TCs and MRG waves in the western Pacific, little can be found pub-

lished in the literature on TC modulation by the equatorial waves.

Thus the advancements to be made by this study are twofold: to document the modulation of TC genesis by the MJO specifically for the south Indian Ocean region west of 100°E, and to document any modulation that may exist in the region by ER, Kelvin, and MRG waves. This is accomplished using a 26-yr record of best-track TC data, together with satellite observations of convection and model analysis data. A fuller description of this data and its nuances is provided in section 2. Subsequent sections discuss the climatology of TCs in the region (section 3), the identification and categorization of the MJO and large-scale equatorial waves (sections 4 and 5), and modulation statistics of the region’s TCs by these waves (section 6). To attempt to attribute the observed modulation, composites of the large-scale environment associated with the waves are studied in section 7. Finally, section 8 is devoted to a summary and discussion.

2. Data and wave-type filtering

This study is restricted to the austral summer season, November through April, in the western and central portions of the south Indian Ocean (west of 100°E). The TC dataset used is that collected and archived by the La Réunion Regional Specialized Meteorological Center (RSMC) for their official region of responsibility (WMO 2002). The period of data we use here is 1979–2004; 1979 was chosen as the beginning year as this represents the time from which the routine use of satellite data allowed for a consistent identification and analysis of TCs. Tropical cyclone genesis is defined by the forecaster as the location at which a named TC is estimated to attain tropical depression status, defined as a system attaining 30-kt 1-min sustained wind speeds and a central pressure of less than 1000 hPa.

For the identification and analysis of the modes of large-scale tropical wave variability, satellite-observed outgoing longwave radiation (OLR) data are used, as is a good proxy for tropical convection. Liebmann and Smith (1996) provide a full description of the data. The daily interpolated OLR is on 2.5° latitude–longitude grid and is continuously available for the same period as the TC dataset.

To isolate the signals of the MJO, Kelvin, ER, and MRG waves from the OLR data, it is decomposed into symmetric and antisymmetric components about the equator, followed by wavenumber–frequency filtering, specifically for each wave. The symmetry constraints and wavenumber–frequency filtering are the same as those used by Wheeler and Kiladis (1999). For the

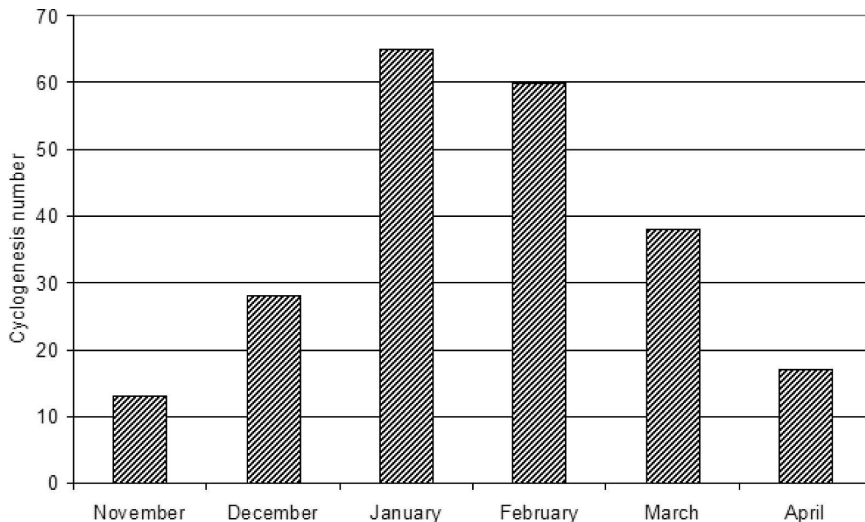


FIG. 1. Number of TC genesis records, stratified by month, during the 1979–2004 period in the domain 0° – 30° S, 35° – 100° E.

Kelvin and ER waves, the symmetric component is used, while for the MRG wave, the antisymmetric component is used. For the MJO no symmetry restriction is made, equivalent to using both antisymmetric and symmetric components. The filtering for the MJO is for eastward propagating planetary wavenumbers 1 through 5, and periods of 30 to 96 days. For the Kelvin, ER, and MRG waves, the filtering retains only the variability occurring for wavenumbers and frequencies lying along and between the theoretical shallow-water dispersion curves corresponding to the equivalent depths of 8 and 90 m. As shown by Wheeler et al. (2000), this method is effective for isolating the convectively coupled wave signals.

Wind field analysis data from the European Centre for Medium-Range Weather Forecasts (ECMWF) are also used. They are available for the same period as the TC data, are on a 1° latitude-longitude grid, and have daily resolution. Data at the 850- and 200-hPa levels are analyzed to investigate the large-scale environment in which the TCs develop.

In section 7, composites are formed of both total and anomaly data. For this, anomalies are created by subtracting the smoothed (with 5-day running mean) 26-yr daily climatology. No other time or spatial filtering is applied to the composited data.

3. Climatology of TC genesis and associated basic state

Before discussing the modulation of TC genesis, it is relevant to have a better understanding of the characteristics of the background flow in which TCs and the large-scale waves occur. It is also useful to know the seasonal and geographical distribution of the recorded TC formations in the region. During November through April, there were 221 named TC genesis events between 35° and 100° E in the 26 yr analyzed. Slightly more than 75% of the classifiable genesis cases were in the January–March period, with the most (65) being in January (Fig. 1). The geographical distribution (Fig. 2)

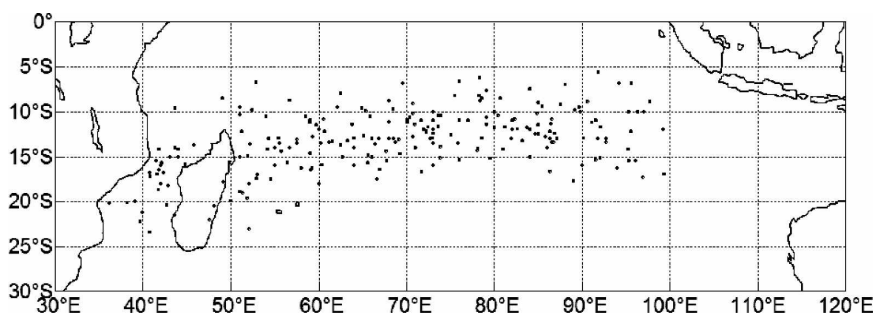


FIG. 2. Geographical distribution of all TC genesis positions (west of 100° E) during the 1979–2004 period.

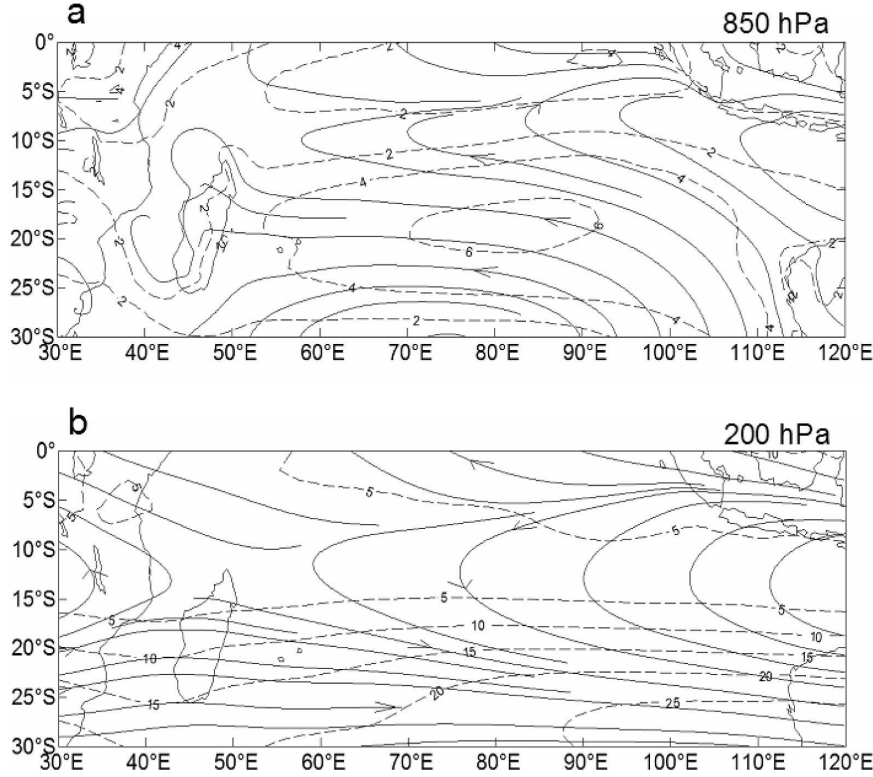


FIG. 3. Summer (November–April) mean isotachs (dashed contours) and streamlines (solid lines) at the (a) 850- and (b) 200-hPa levels. Contour interval for isotachs is 2 m s^{-1} in (a) and 5 m s^{-1} in (b).

exhibits two relatively distinct areas where genesis is favored: the Channel of Mozambique, and the central south Indian Ocean, on either side of the island of Madagascar, in the $5^{\circ}\text{--}25^{\circ}\text{S}$ band.

As mentioned in section 1, the formation and life cycle of TCs have previously been related to thermodynamic and dynamic conditions of the large-scale environment. Focusing on the dynamical aspects of the basic-state flow, summer (November–April) mean lower and upper-level wind fields are displayed in Fig. 3. The flow at 850 hPa (Fig. 3a) shows the Mascareigne anticyclone, centered at 30°S , 75°E . On the equatorward side of the anticyclone is a broad region of south-easterly trade winds with maximum speeds around $15^{\circ}\text{--}20^{\circ}\text{S}$. Cross-equatorial monsoon flow is present in the $0^{\circ}\text{--}5^{\circ}\text{S}$ latitude band, with the monsoon trough, indicated by cyclonically curving flow, existing around 10°S . At the upper level (Fig. 3b), 200-hPa streamlines indicate the occurrence of westerlies poleward of 15°S , easterlies north of 10°S , and recurving flow in between. Overall, Figs. 2 and 3 indicate that the geographical position of TC genesis is, on average, located just poleward of the low-level monsoon trough and is collocated with the recurving flow in the upper troposphere. Con-

sistent with numerous previous studies (e.g., Gray 1968; McBride and Zehr 1981; McBride and Keenan 1982), the TC genesis locations are in an area of climatological low-level cyclonic vorticity, and weak vertical wind shear (Fig. 4). Indeed, both the mean latitude of TC genesis, and these two climatological parameters, consistently show a slight southward shift as one moves west in the region.

4. Identification of the large-scale waves

As discussed in section 2, the initial identification of the modes of large-scale tropical wave variability is made using symmetry-specified, wavenumber-frequency filtered, OLR. This procedure produces Tropic-wide ($20^{\circ}\text{S}\text{--}20^{\circ}\text{N}$) maps of OLR anomalies each day for each wave mode. To restrict further our consideration to the region of interest, and to reduce the dimensionality of the data required to represent each wave, empirical orthogonal function (EOF) analysis was performed upon the filtered fields over a restricted domain. In subsequent sections, the temporal coefficients from the EOF analyses will be used as an index measure of each wave. Such an analysis also serves the

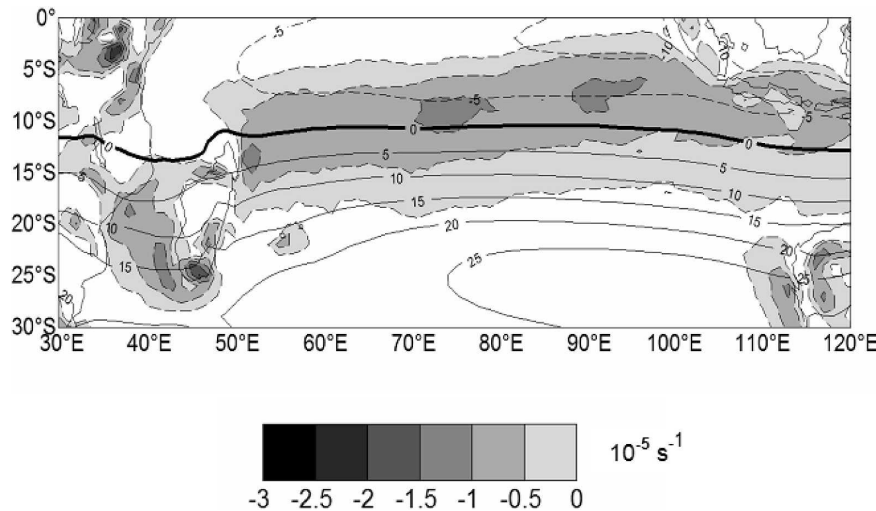


FIG. 4. Summer (November–April) mean vertical shear of the zonal wind (200-hPa zonal wind minus 850-hPa zonal wind; solid contours) and 850-hPa vorticity (shading). Contour interval for vertical shear is 1 m s^{-1} . Only negative vorticity is shown, with a scale provided.

purpose of showing the structure of each wave in the region, and providing its propagation properties.

For the MJO, the EOF analysis was performed in the domain 20°S – 20°N , 0° – 357.5°E .¹ Consistent with previous studies (e.g., Matthews 2000), the leading two EOFs are a pair in approximate quadrature, representing the eastward propagation of the MJO (Fig. 5). The spatial structures of this leading EOF pair (Figs. 5a and 5b) reproduce well those of many previous studies (e.g., Slingo et al. 1999; Lo and Hendon 2000; Matthews 2000), giving confidence that an index developed from the principal component (PC) time series will adequately measure the MJO. The (normalized) PC time series for a portion of the record are shown in Fig. 5c. A lagged correlation analysis (not shown) yields the result that PC1 leads PC2 by an average of 11 days, giving an estimated eastward phase speed of 4.6 m s^{-1} over the Indian Ocean.

For the $n = 1$ ER wave, given its characteristically smaller zonal spatial scale than the MJO (Wheeler et al. 2000), a smaller domain (20°S – 20°N , 30° – 120°E) was chosen for the EOF analysis (Fig. 6). The leading two EOFs form a quadrature pair, and represent the westward propagation of the ER wave along the equator with PC1 leading PC2. By definition (section 2), the spatial structures are symmetric about the equator. The spatial patterns exhibit maxima at 10° of latitude, consistent with the structure for ER waves produced by

Wheeler et al. (2000). The estimated average westward phase speed from the lag relationship of the PCs is 5 m s^{-1} (not shown).

The leading two EOFs for the analysis of the Kelvin wave-filtered OLR, limited to the same domain as that for the ER wave, are presented in Fig. 7. They too form a quadrature pair, with the implied propagation being eastward (PC2 leads PC1). The maximum anomaly of -8 W m^{-2} is directly on the equator (Fig. 7b), in contrast to the slightly off-equatorial maxima for the MJO (Figs. 5a and 5b). The estimated average speed of propagation from the lag of the PCs is 16 m s^{-1} (not shown).

Finally, the leading EOFs from the analysis of the MRG wave-filtered OLR, limited to the same domain as used for the ER and Kelvin waves, is presented in Fig. 8. They form a pair in approximate quadrature with EOF1 leading EOF2, implying westward propagation. The equatorial antisymmetric anomalies are maximized at 7.5°S and 7.5°N , consistent with the geographical distribution of MRG wave variance found by Wheeler and Kiladis (1999). The estimated average westward phase speed from the lag relationship of the PCs is 26 m s^{-1} (not shown).

5. Category definitions of the large-scale waves

To analyze the modulation of TCs by the large-scale wave variability, it is useful to define a number of categories of each wave to represent their state over the domain at any particular time. We do this by dividing the phase space spanned by the vector (PC1, PC2) into

¹ All EOF analyses were conducted on the covariance matrix of the data.

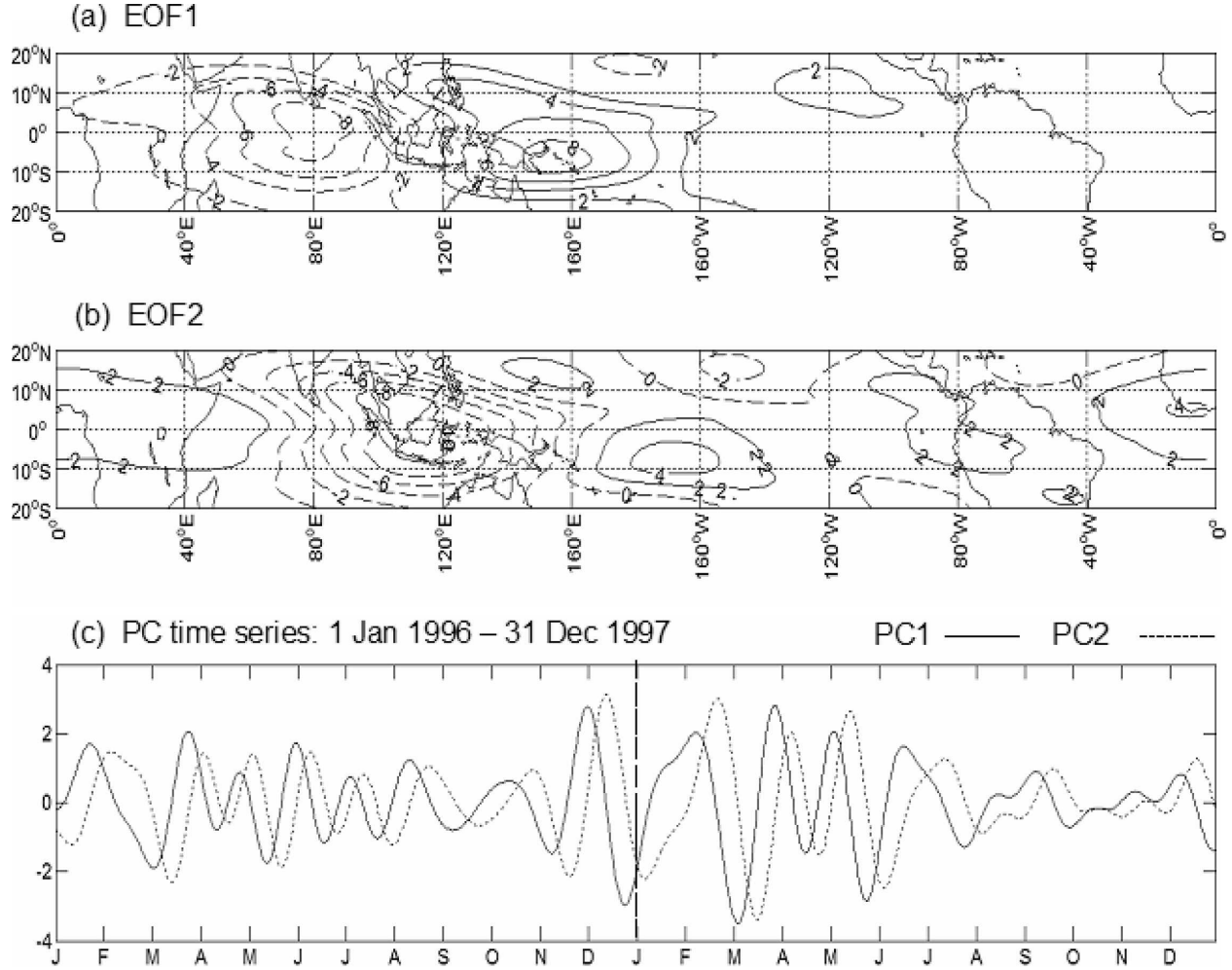


FIG. 5. First two EOFs of the MJO wavenumber–frequency filtered OLR: (a) EOF1 (accounting for 17% of the filtered variance) and (b) EOF2 (17%). Contour interval is 2 W m^{-2} with the zero contour omitted. (c) PC1 (solid line) and PC2 (dotted line) showing a subset of the series from 1996 to 1997 only.

six (equal angle) categories, as demonstrated for the MJO in Fig. 9. Such an EOF phase-space representation has previously been successfully used (e.g., Hall et al. 2001). In Fig. 9, the MJO is strong when the (PC1, PC2) point traces large-radius anticlockwise circles (EOF1 leads EOF2 for the MJO). In category 1, PC1 is positive and PC2 is near zero. In category 2, both PC1 and PC2 are positive, and so forth. For a typical complete cycle of the MJO, all six categories occur in sequential order.

As well as the six “active” categories, a “weak,” or “category 0,” is defined to occur at times when the amplitude of the (PC1, PC2) vector, that is, $(\text{PC1}^2 + \text{PC2}^2)^{1/2}$, is less than 1.0, as also shown for the MJO phase space in Fig. 9.

Categories are defined in the same way for each of the other large-scale waves, except using PC1 and PC2

from their own respective EOF analyses. Thus for each wave there exists a single category for each day.

6. Statistics of regional TC genesis modulation

As a first step in this study of TC modulation, we apply a binning procedure whereby each individual TC is assigned to the wave category that was operating at the time of its formation. As described above, one of seven categories is assigned for each wave, six “active” categories plus the weak category (category 0). The number of TC formations occurring in each category may then be compared to assess whether modulation is occurring, and a statistical test applied to determine the significance of the result. Initially, the binning is performed using TCs from the whole domain, that is, 35° to 100°E (Table 1). Obviously, as the region is 65° in lon-

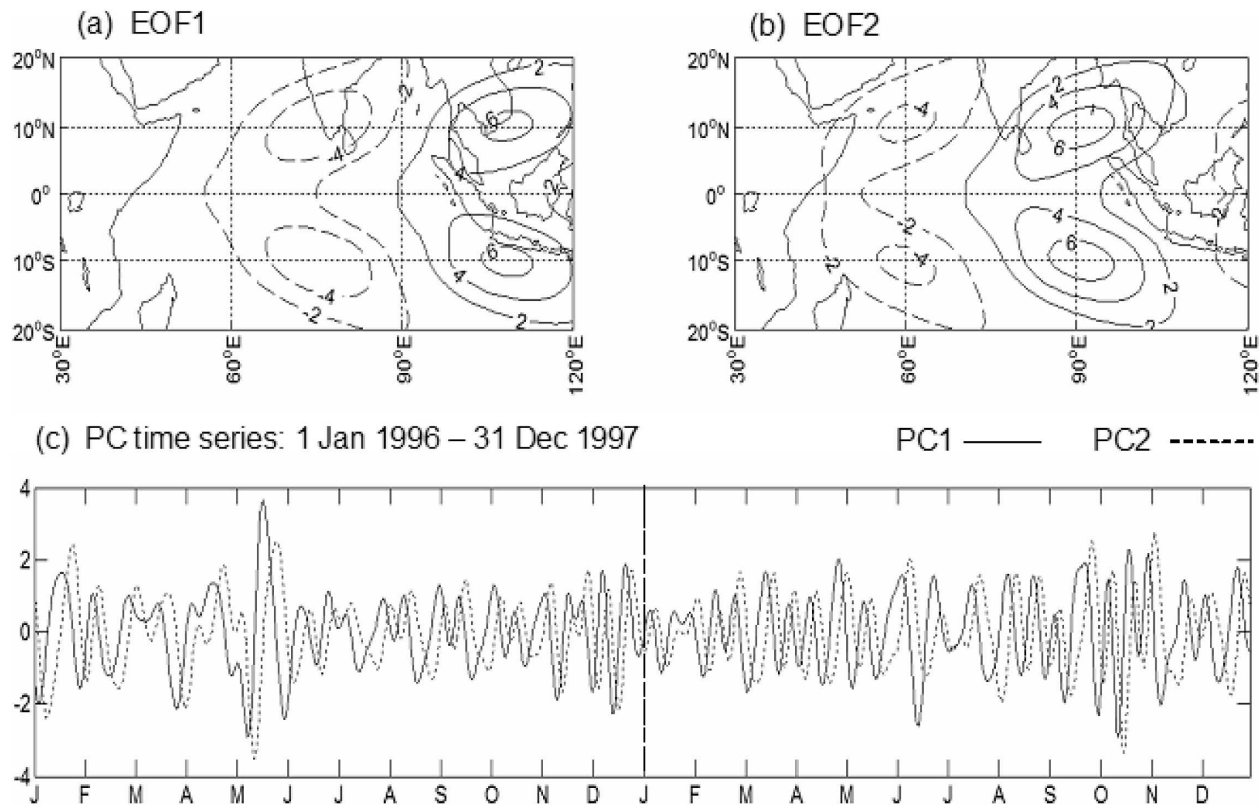
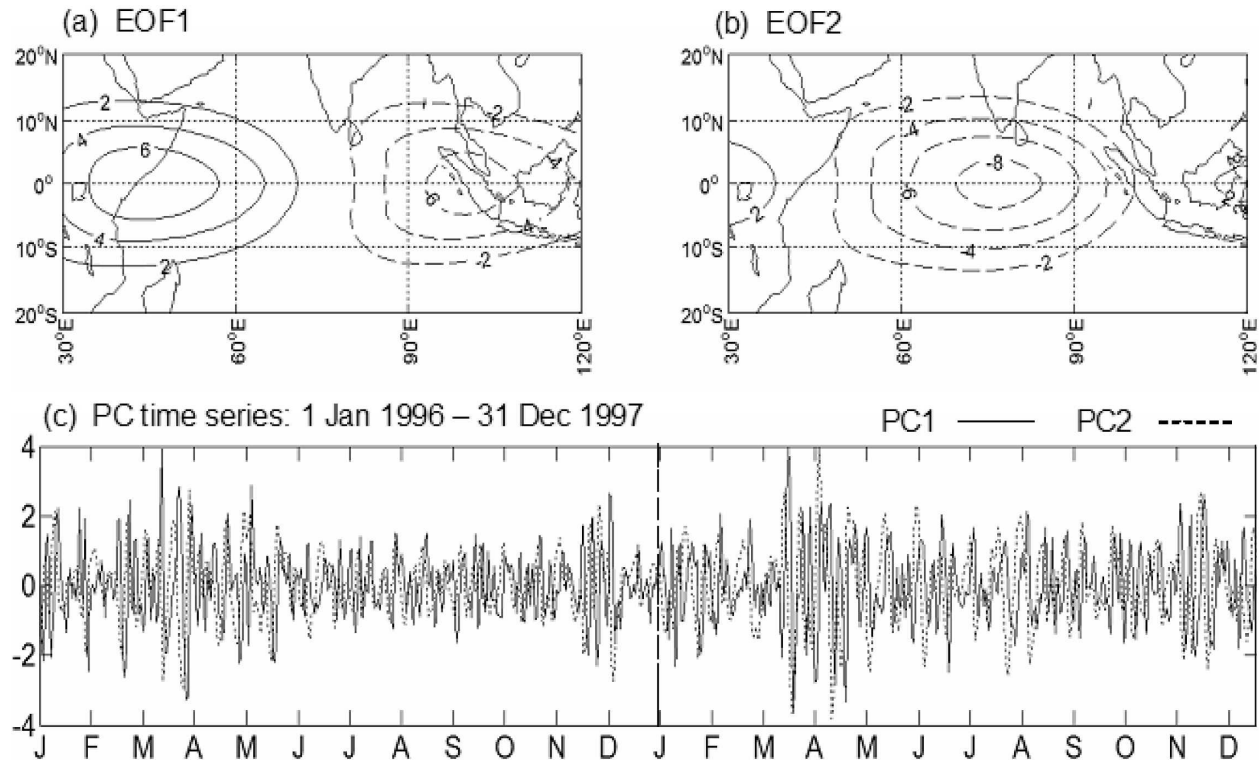
FIG. 6. As in Fig. 5, but for the $n = 1$ ER wave-filtered data: (a) EOF1 (20%) and (b) EOF2 (18%).

FIG. 7. As in Fig. 5, but for the Kelvin wave-filtered data: (a) EOF1 (18%) and (b) EOF2 (17%).

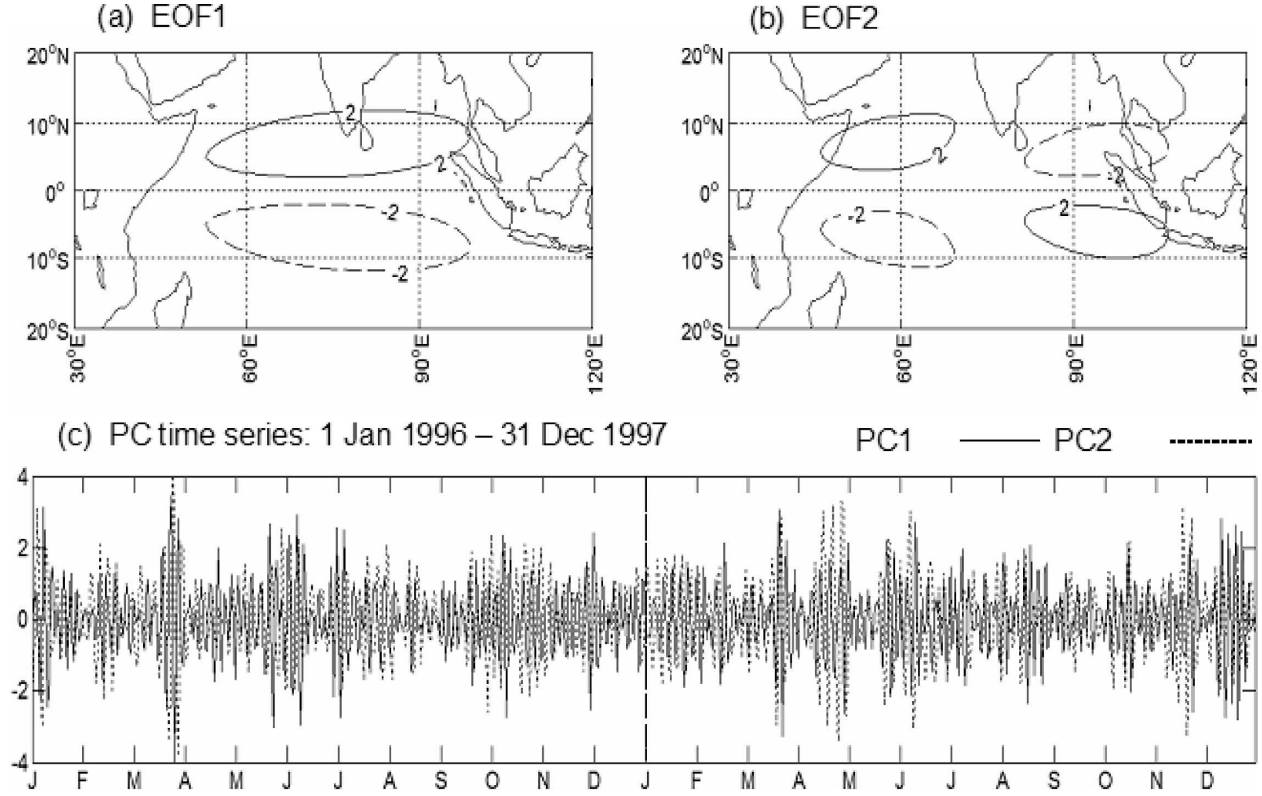


FIG. 8. As in Fig. 5, but for the MRG wave–filtered data: (a) EOF1 (15%) and (b) EOF2 (12%).

gitude wide, this analysis will only have the possibility to show a significant result if the modulation by the large-scale wave variability is operating with a rather large zonal spatial scale (i.e., a spatial scale with large projection onto a 65° zone). Noting the size of the OLR anomalies associated with the waves (Figs. 5–8), the domain's size is likely well suited to the scale of the MJO and Kelvin wave, but may be somewhat too large for smaller-scale waves. Thus if we fail to find a significant modulation by a wave in the whole domain, we look further for a modulation in western and eastern subdomains (Table 2).

The binning procedure follows that applied by Hall et al. (2001), in their study of TC modulation over the Australian region. Also following Hall et al. (2001) is the statistical test we apply to test whether each category has significantly more or fewer TCs than expected. The null hypothesis is that the TCs should be spread among the categories proportionally to the number of days in each category, that is, no modulation. The test statistic, as computed separately for each category, is

$$Z = \frac{\hat{p} - p_0}{\sqrt{p_0(1 - p_0)/N}},$$

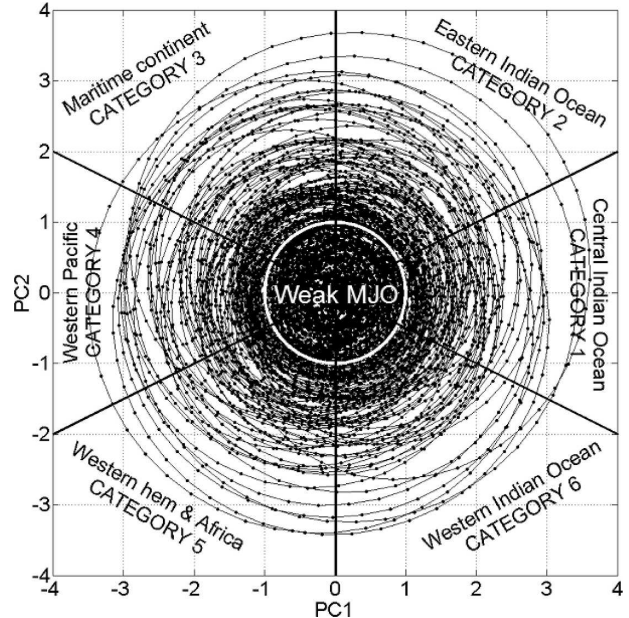


FIG. 9. PC1–PC2 phase-space points of November–April MJO activity during 1979 to 2004. Six equal-angled phase-space categories are defined, together with a region indicating weak wave activity. For each category, the approximate locations of the enhanced convective signal of the MJO are also labeled.

TABLE 1. Summary of wave and TC genesis statistics. The second column lists the number of days for which the specified wave was in the specified category. This is also expressed as a percentage of the total number of days (third column). In the fourth column, the “Number” refers to the number of TCs that formed within the category, as is also expressed as a percentage of the number of days in that category (the daily genesis rate; fifth column). Categories where TC genesis numbers were significantly above (below) average at the 95% level are indicated by * (**).

MJO category	MJO day		TC genesis	
	Number	Percentage	Number	Percentage
1	523	11.4	25	4.8
2	566	12.3	40*	7.1*
3	528	11.5	19	3.6
4	519	11.3	22	4.2
5	515	11.2	14**	2.7**
6	508	11.1	24	4.7
0	1432	31.2	77	5.4
Total	4591	100	221	4.8
ER category	ER day		TC genesis	
	Number	Percentage	Number	Percentage
1	463	10.1	35*	7.6*
2	441	9.6	18	4.1
3	460	10.0	19	4.1
4	462	10.1	13**	2.8**
5	457	10.0	19	4.2
6	455	9.9	20	4.4
0	1853	40.4	97	5.2
Total	4591	100	221	4.8
Kelvin category	Kelvin day		TC genesis	
	Number	Percentage	Number	Percentage
1	378	8.2	19	5.0
2	463	10.1	32*	6.9*
3	478	10.4	24	5.0
4	355	7.7	13	3.7
5	498	10.8	17	3.4
6	485	10.6	18	3.7
0	1934	42.1	98	5.1
Total	4591	100	221	4.8
MRG category	MRG day		TC genesis	
	Number	Percentage	Number	Percentage
1	430	9.4	19	4.4
2	439	9.6	25	5.7
3	442	9.6	26	5.9
4	442	9.6	22	5.0
5	442	9.6	21	4.8
6	444	9.7	19	4.3
0	1952	42.5	89	4.6
Total	4591	100	221	4.8

where \hat{p} and p_0 are the observed and expected fraction of days for which a TC forms, and N is the number of days in the category. Given the null hypothesis, the “expected” fraction of cyclogenesis days is given by the total number of TCs divided by the total number of

TABLE 2. As in Table 1 except for the MRG wave over western and eastern Indian Ocean subdomains.

MRG category	Western Indian Ocean (30°–75°E)			
	MGR day		TC genesis	
	Number	Percentage	Number	Percentage
1	430	9.4	11	2.6
2	439	9.6	18	4.1
3	442	9.6	16	3.6
4	442	9.6	17	3.8
5	442	9.6	11	2.5
6	444	9.7	7	1.6
0	1952	42.5	58	3.0
Total	4591	100	138	3.0
MRG category	Eastern Indian Ocean (75°–120°E)			
	MGR day		TC genesis	
	Number	Percentage	Category	Number
1	430	9.4	8	1.9
2	439	9.6	7	1.6
3	442	9.6	10	2.3
4	442	9.6	5	1.1
5	442	9.6	10	2.3
6	444	9.7	12	2.7
0	1952	42.5	31	1.6
Total	4591	100	83	1.8

days, that is, 4.8% when expressed as a percentage for the whole domain (Table 1), and 3.0% and 1.8% for the western and eastern domains respectively (Table 2). Using a two-tailed test, critical values of Z for 95% significance are ± 1.96 . Note that we compute the daily TC genesis rate percentages irrespective of whether more than one TC formed on a single day.

As presented in Table 1, the MJO, ER, and Kelvin waves each have at least one category in which the null hypothesis is rejected at the 95% level for TCs binned across the whole domain. For the MJO, significantly more TCs formed than expected in category 2 (7.1% daily genesis rate), and significantly fewer in category 5 (2.7% daily genesis rate). This amounts to a modulation of about 2.6 to 1 by the MJO in this large domain. For the ER wave, it is category 1 that has significantly more TCs than expected (7.6% genesis rate), and category 4 that has fewer (2.8% genesis rate), resulting in a modulation of about 2.7 to 1. For the Kelvin wave, on the other hand, the null hypothesis is rejected in only one category; category 2 has a daily genesis rate of 6.9%, significantly more than the normal rate of 4.8%. Compared to the category with the lowest rate, this amounts to a modulation of about 2 to 1 for the Kelvin wave. No statistically significant (even at the 90% level) modulation of near-basinwide TCs is found for the MRG wave.

While the above result suggests that MRG waves

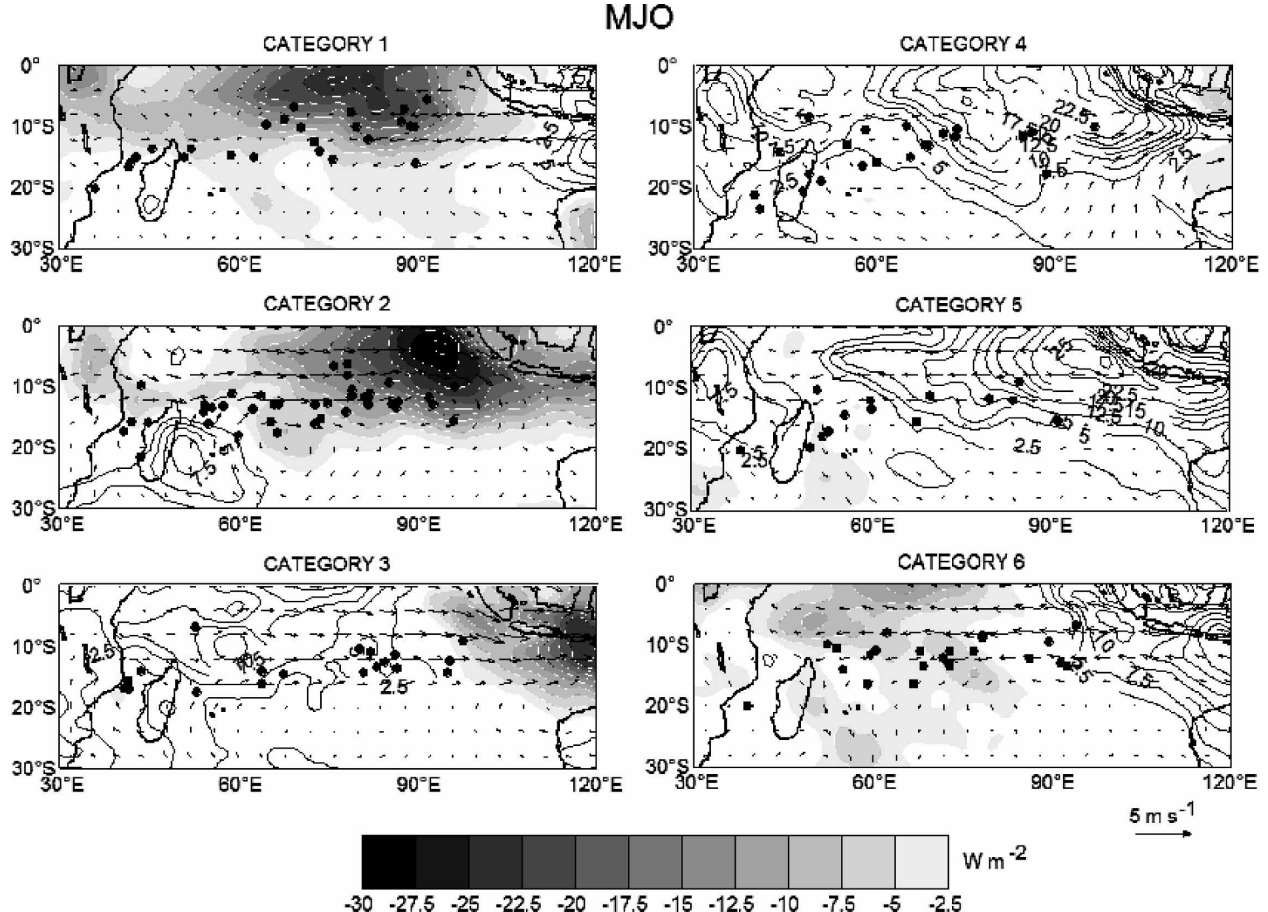


FIG. 10. Composite 850-hPa wind anomalies (vectors) and unfiltered OLR anomalies (shading for negative values and solid contours for positive values) for each category of the MJO. Contour interval for the OLR is 2.5 W m^{-2} with the zero contour omitted. The TC genesis locations in each category are also plotted (solid circles).

have little influence, it is still possible that a modulation by MRG waves may exist in a smaller region. We have investigated this by dividing the full domain into western and eastern subdomains at the longitude of 75°E . Given the spatial scale of the MRG waves, as suggested by Fig. 8, this new domain size may be more suitable for diagnosing an influence, should one exist. The results are summarized in Table 2. Although relatively large variations in the cyclogenesis rate can be discerned (e.g., category 2 compared to category 6), there is still no category for which the threshold for 95% statistical significance is reached.

To summarize thus far, we have been able to show a relatively large and significant modulation of TCs in the region by the MJO and ER waves, a small yet significant modulation by Kelvin waves, and a modulation by MRG waves that is not significant. These results thus warrant further investigation. Of particular interest are the modification of the large-scale environment by the

waves and the attribution of the above-described TC modulation to that modified environment.

7. Large-scale wave composites and attribution of TC modulation

Throughout the literature, there has been a preponderance of studies associating TC development with large-scale conditions of the environment (e.g., Gray 1968, 1979; McBride and Zehr 1981; Frank 1987; Merrill 1988; Landsea et al. 1998). Gray (1968, 1979) studied the climatological distribution and seasonality of TC genesis around the globe, and found there were a number of necessary conditions. Frank (1987) summarized them as follows: warm sea surface temperatures coupled with a relatively deep oceanic mixed layer; significant values of absolute vorticity in the lower troposphere; weak vertical wind shear over the prestorm disturbance; and mean upward motion and high midlevel

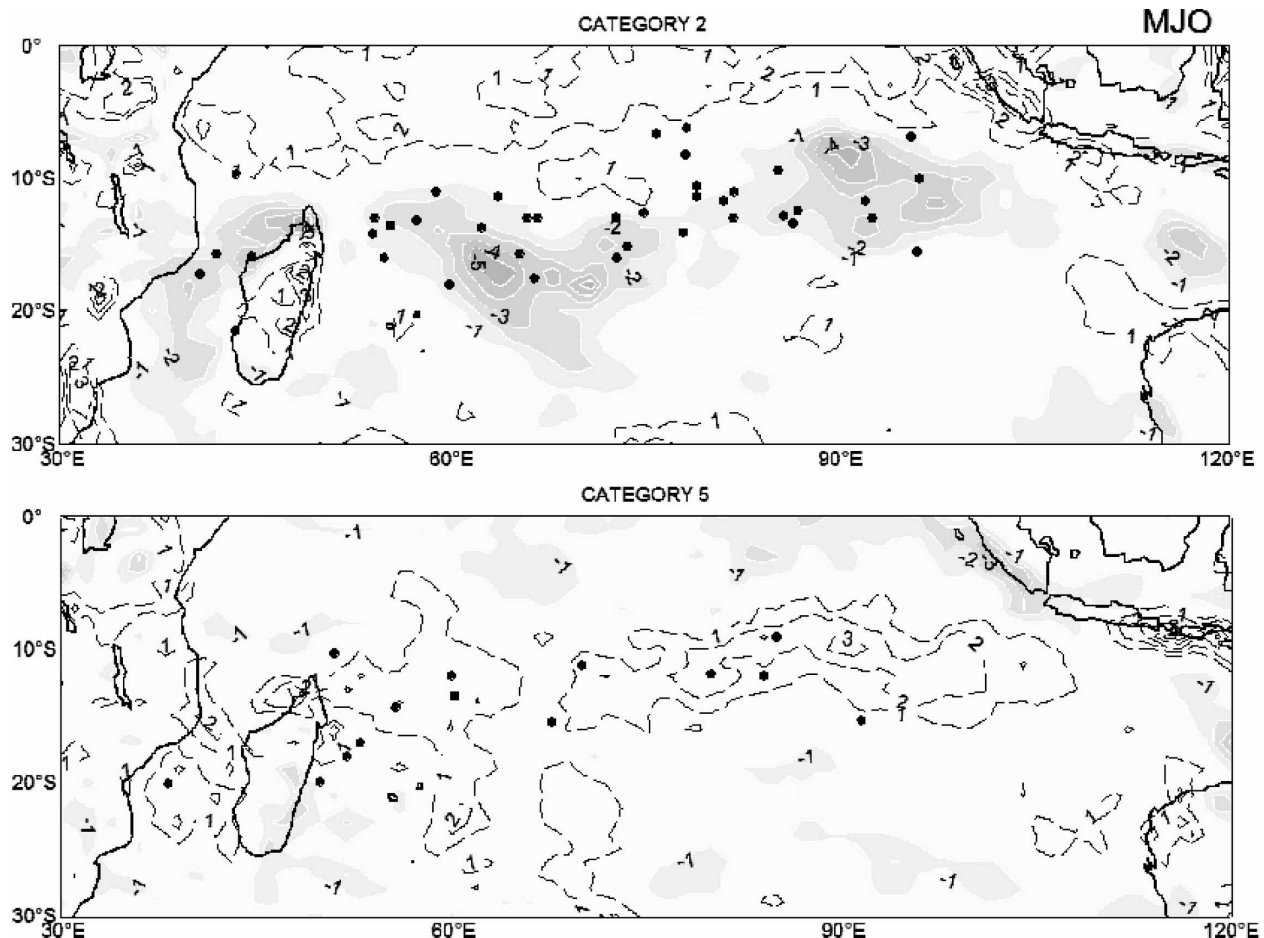


FIG. 11. As in Fig. 10, except for composite 850-hPa vorticity anomalies for categories 2 and 5 of the MJO only. Contour interval is $1.0 \times 10^{-6} \text{ s}^{-1}$ with negative values shaded and positive values presented as dashed contours.

humidities. As noted in section 1, variations in the two dynamic conditions, that is, the low-level vorticity and vertical wind shear, have since been shown to be relevant for explaining *subseasonal* TC variability as well, either in relation to modulation by the MJO (Maloney and Hartmann 2000b; Hall et al. 2001) or in relation to the development of individual systems (McBride and Zehr 1981). The thermodynamic conditions, that is, warm sea surface temperatures, a deep oceanic mixed layer, and moist air in the midtroposphere, on the other hand, have previously been reported to be generally satisfied for long periods of the year (McBride and Zehr 1981; Frank 1987), and consequently usually neglected in studies of subseasonal TC variability. Yet Kemball-Cook and Weare (2001) found significant midtropospheric humidity variations associated with the MJO. Despite this, we too have chosen to neglect the thermodynamic conditions, an important caveat of the study.

For attribution of the TC modulation observed in this

study, we thus look at the fields of 850-hPa vorticity and vertical shear of the zonal wind between the 200- and 850-hPa levels. The 850-hPa vorticity is qualitatively representative of that of the whole of the lower troposphere. For the shear calculation, only the zonal wind is presented because changes to the shear of the meridional wind are found to be negligible by comparison. Additionally, OLR is studied because of the need for a preexisting convective disturbance from which a TC can develop (Frank 1987). Anomalies of OLR are well related to the amount of deep convective activity in an area (e.g., Arkin and Ardanuy 1989), and it is adequate to assume that large-scale time-averaged anomalies of OLR are a good proxy for the number and strength of individual synoptic to mesoscale convective disturbances making up that anomaly (e.g., Hendon and Liebmann 1994).

The approach we take is to compute composites of the fields for each category of each of the large-scale waves. Composites of either total or anomaly fields are

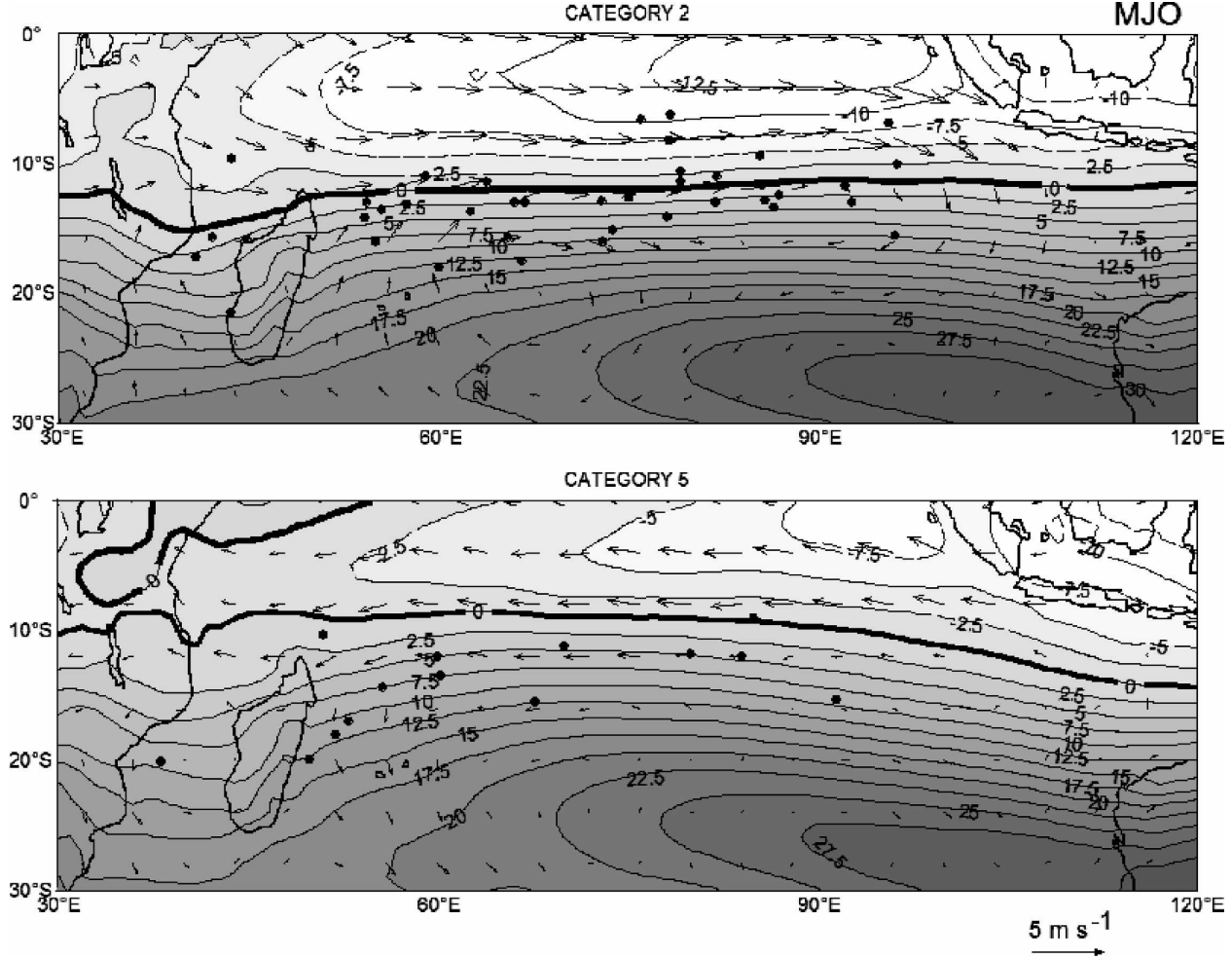


FIG. 12. As in Fig. 11, except for composite 850-hPa wind anomalies (vectors) and vertical zonal wind shear (zonal wind at the 200-hPa level minus zonal wind at the 850-hPa level; contours). Contour interval is 2.5 m s^{-1} with a thick line delineating the zero contour.

studied. Anomalies are computed by subtracting the smoothed (with 5-day running mean) 26-yr daily climatology. No spatial or time filtering is applied to the composited data.

a. MJO

Figure 10 presents the composite OLR anomalies and 850-hPa wind anomalies for the MJO, with the locations of TC genesis for each category superimposed. The signal of the MJO in convection and low-level winds is as expected (e.g., Sperber 2003; Wheeler and Hendon 2004), with coupled patterns of wind and convection moving slowly eastward. The adequacy of the method of identifying the MJO, and of compositing, is thus confirmed.

Consistent with Table 1, the highest rate of domain-averaged TC genesis occurs in category 2, and the least in category 5 (Fig. 10). The increased genesis occurs at

a time when the MJO is producing anomalous westerlies equatorward of 15°S , across the whole Indian Ocean, and enhanced convection in the east of the domain. Conversely, category 5 of the MJO has near-equatorial easterly anomalies, with suppressed convection shifted somewhat to the east.

The vorticity anomalies of categories 2 and 5 of the MJO are presented in Fig. 11. The correspondence between the vorticity anomalies and the locations of TC genesis is quite high; better than that observed for the OLR in Fig. 10, with negative vorticity anomalies predominating around the TC locations in category 2. This suggests a more dominant role of the vorticity for the TC modulation. Further, the magnitude of the vorticity anomalies is quite large, being of comparable magnitude to the season-mean values (e.g., Fig. 4).

Of course, there is always the question of whether the composite anomalies are a result of the TCs

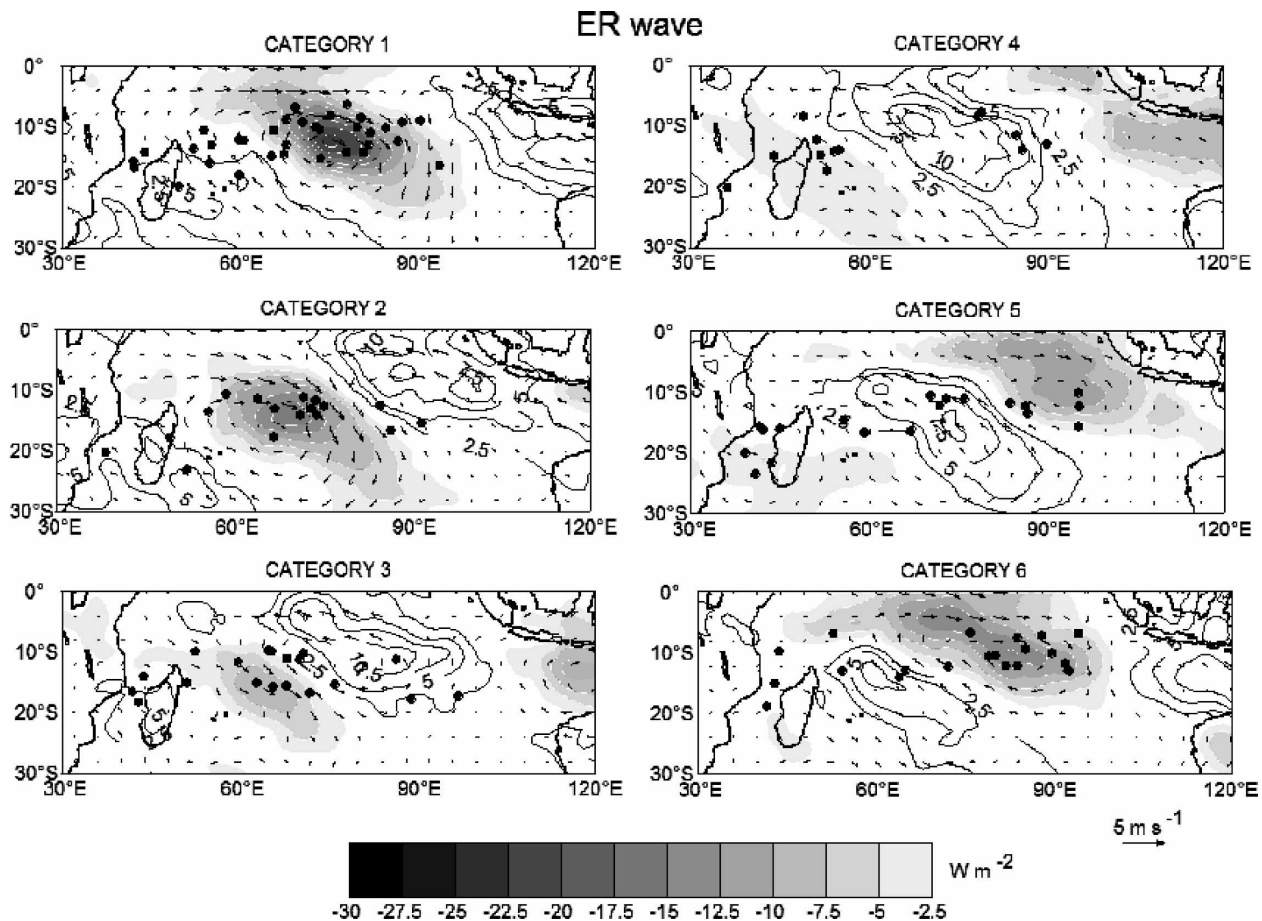


FIG. 13. As in Fig. 10, but for the ER wave.

themselves. Certainly, the TCs can account for some of the anomalies, but given that there are more than 500 days of data going into each composite (Table 1), and only 40 (in category 2) or 14 (in category 5) TCs being included across the whole domain, the extent to which the TCs can affect the composites is limited.

Relatively large changes in the vertical shear of the zonal wind between categories 2 and 5, especially near 60°E, are also observed (Fig. 12). The location of the line of zero vertical shear, as is usually located near 10°S in the mean (e.g., Fig. 4), shifts from being at around 12°S in category 2 to 9°S in category 5. The location of the zero line during category 2, with large positive zonal shear poleward, and large negative zonal shear equatorward of the TCs, is entirely consistent with what has previously been observed (e.g., McBride and Zehr 1981) and modeled (e.g., Wong and Chan 2004) to be favorable for TC development. Changes in the vertical shear of the meridional wind, by comparison, are negligible (not shown).

Thus the large modulation of TC genesis in the region by the MJO seems attributable to both the influence of the MJO on the low-level vorticity, and the vertical wind shear. The MJO's modulation of deep convective activity and imbedded convective disturbances, for which we have used OLR as a proxy, appears to be comparatively less important.

b. ER wave

Composite 850-hPa wind and OLR anomalies for every category of the ER wave are presented in Fig. 13. The westward-propagating off-equatorial centers of convection, as are coupled to off-equatorially centered circulation cells, look consistent with what has been indicated for this wave elsewhere (e.g., Wheeler et al. 2000). At the time of the maximum rate of TC genesis, that is, category 1 (Table 1), enhanced convection (negative OLR anomalies) and cyclonic circulation anomalies, are centered in the domain of study. Throughout the depicted evolution, the TC genesis lo-

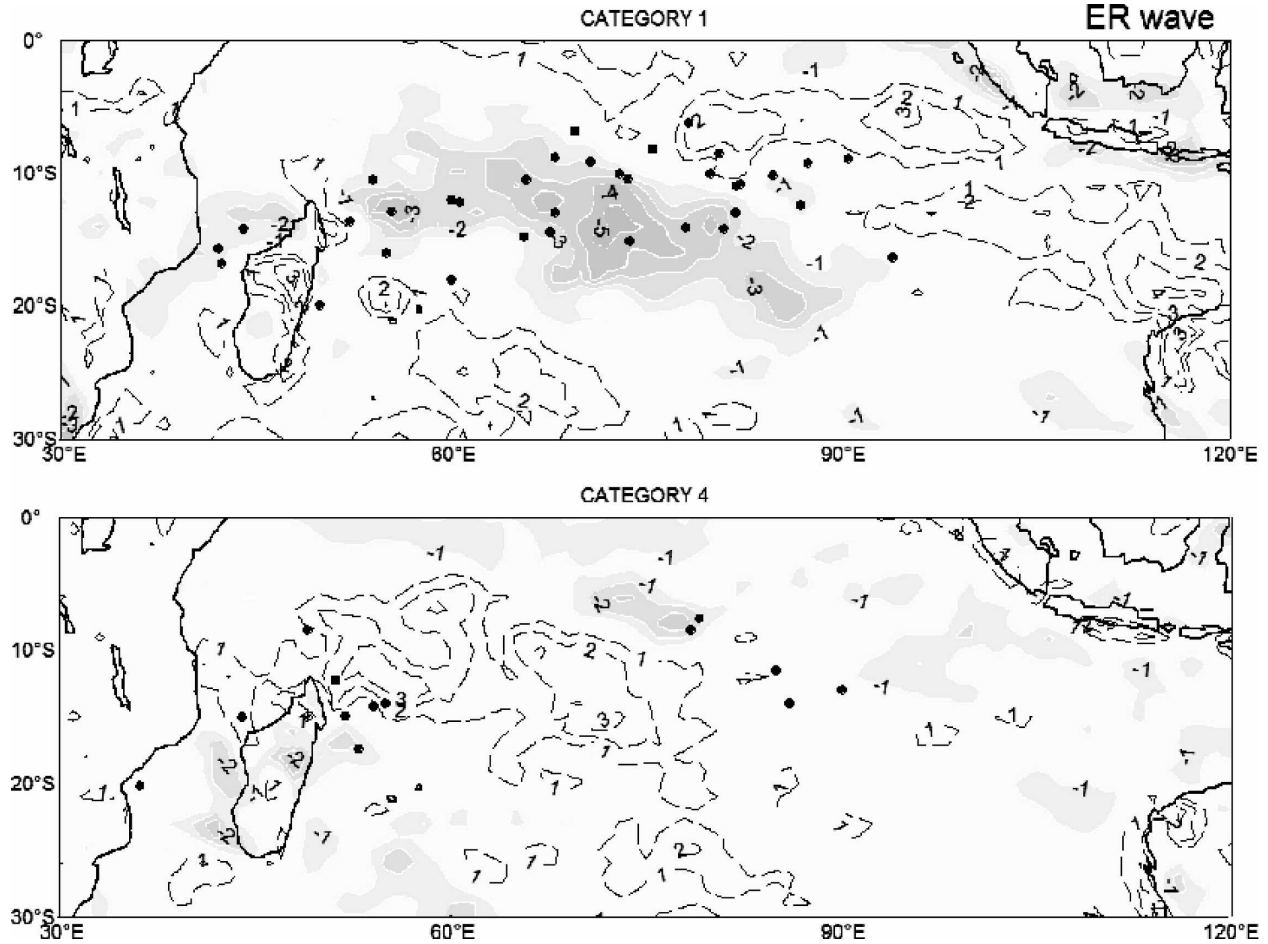


FIG. 14. As in Fig. 11, but for categories 1 and 4 of the ER wave.

cations appear most concentrated about the center of the large-scale convection and cyclonic circulation cells of the ER wave, and appear to move systematically westward with it.

The 850-hPa vorticity anomalies during categories 1 and 4 of the ER wave are presented in Fig. 14. The very close relation between the large-scale vorticity anomalies of the ER wave, and the TC genesis locations, is revealed. Further, as for the MJO, the magnitude of the vorticity anomalies is quite large, being comparable to the season-mean values.

Differences in the vertical shear between categories 1 and 4 of the ER wave are not large (Fig. 15). Only a small shift in the line of zero vertical shear can be discerned. During category 1, however, the gradient in the vertical shear is stronger, with large positive values just to the south of the zero line, and large negative values to the north. The configuration of the vertical shear during category 1 would thus still be considered as more favorable for TC development.

Thus the large modulation of TCs by ER waves in the

region appears most readily attributable to the large variations in low-level, off-equatorial vorticity by the wave, and its coincidence with supporting variations in convection. The relatively smaller changes in vertical wind shear of the wave, while still supportive of a modulation of TCs, appear to be relatively less important.

c. Kelvin wave

As concluded in the previous section, the Kelvin wave provides only a small, yet statistically significant, modulation of TCs. Category 2 of the Kelvin wave has the highest domain-averaged TC genesis rate, and category 5 the least (Table 1). The 850-hPa wind and OLR anomalies just for these two categories are displayed in Fig. 16. Any relationship between the OLR anomalies and the clustering of TCs is difficult to discern, except that, as for the MJO, the highest number of TCs occur when the enhanced convection of the Kelvin wave is situated over the eastern Indian Ocean. Although the

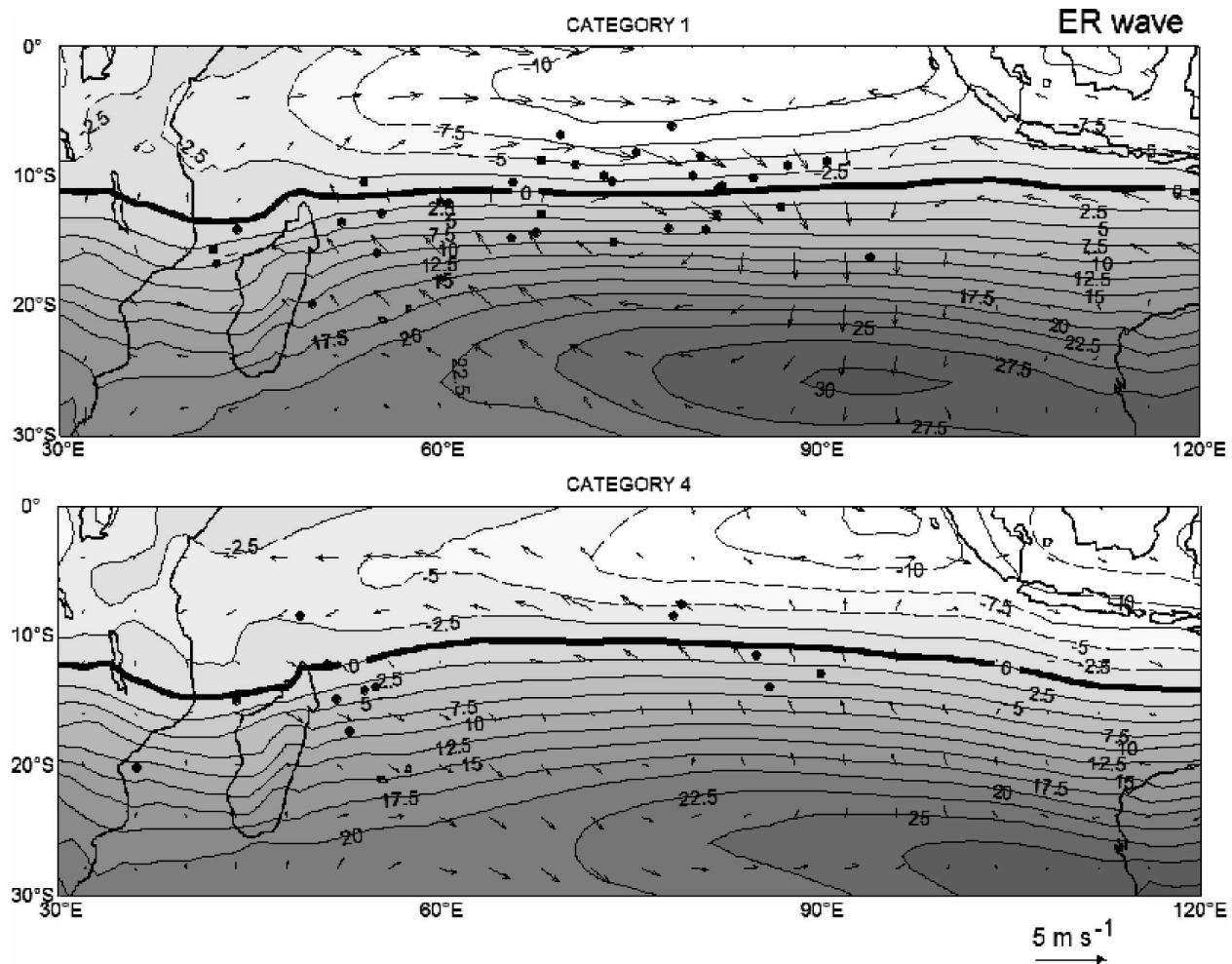


FIG. 15. As in Fig. 12, but for categories 1 and 4 of the ER wave.

signal of the Kelvin wave in the wind field is weaker than that of the MJO or ER wave, the tendency for easterly near-equatorial winds to be associated with fewer TCs, as was the case for the MJO, is also observed.

The 850-hPa vorticity anomalies of the two contrasting categories of the Kelvin wave are displayed in Fig. 17. As for the OLR, no strong relationship is apparent, except that there is a slight tendency for more negative vorticity anomalies along the latitude of 10°S in category 2 compared to category 5. This slight difference in the vorticity is in the correct direction for the observed difference in TCs, and thus may be sufficient for the relatively small TC modulation observed for this wave.

d. MRG wave

Although the modulation indicated in the previous section for the MRG wave did not pass our test of

statistical significance, for completeness we include some analysis of its large-scale circulation in Fig. 18. In the two categories shown, the large-scale signature of MRG waves, which have strong meridional flow across the equator, and near-equatorially centered circulation cells, can be seen, and consistent with previous studies of this wave (e.g., Wheeler et al. 2000), enhanced convection is generally collocated with the poleward low-level flow.

Category 6 is when the MRG wave was found to be associated with the least number of TCs in the western part of the domain (Table 2), and the greatest number in the east. During this category, the large-scale flow of the composite shows strong northerly flow from across the equator to about 15°S around the longitudes of highest cyclogenesis (i.e., around 90°E; Fig. 18), coincident with a region of enhanced convection. Assuming that this convective signature is related to the existence of more “preexisting convective disturbances,” and this

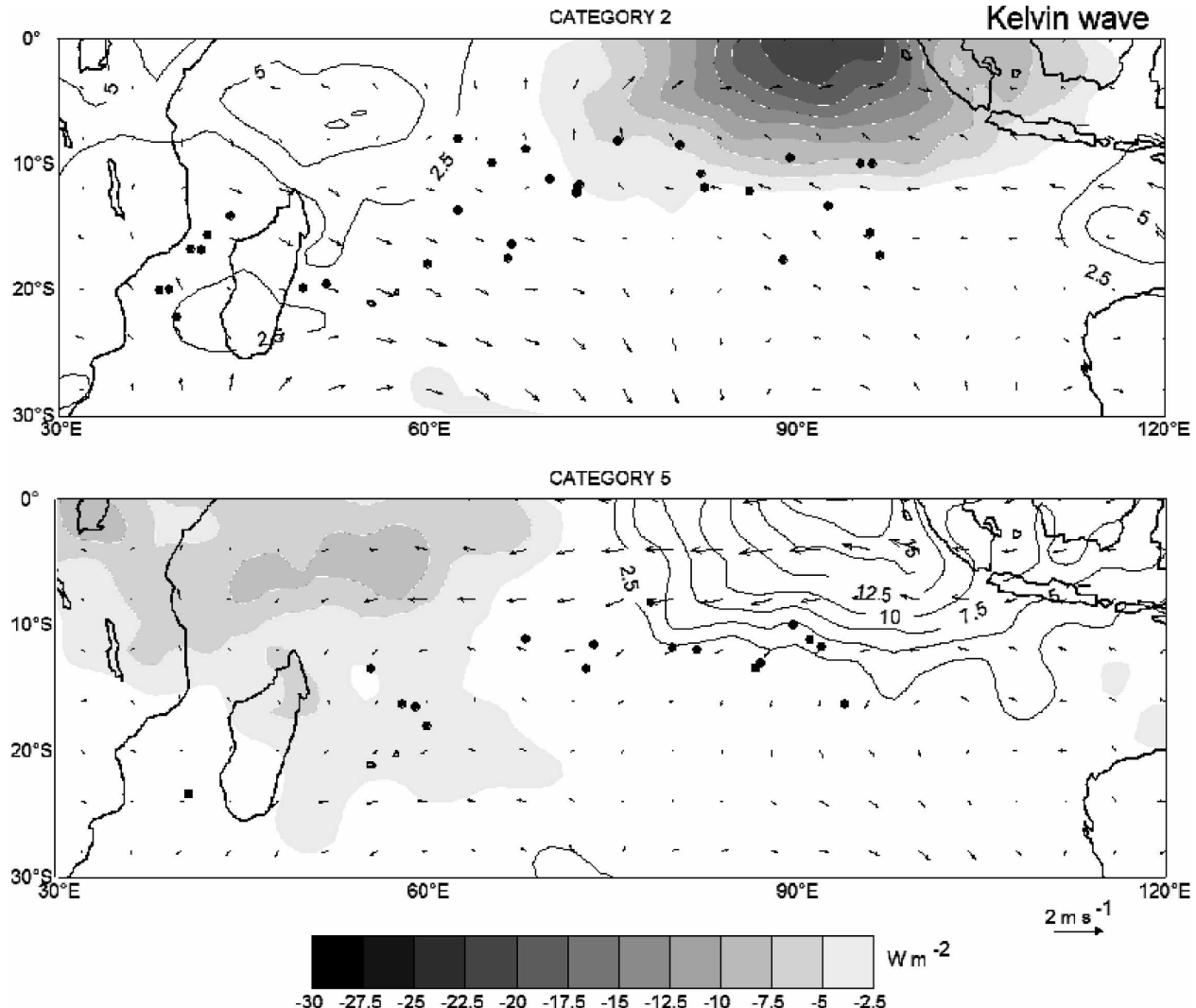


FIG. 16. As in Fig. 10, but for categories 2 and 5 of the Kelvin wave.

is sufficient to produce a modulation of TCs, this large-scale signal of the MRG wave is consistent with the modulation that was found.

8. Summary and discussion

Our aim in this study has been to document and increase understanding of the subseasonal modulation of TC genesis. We focused specifically on TCs over the south Indian Ocean west of 100°E, and the modulation by various large-scale modes of tropical wave variability. In analyzing the statistics of TCs in the region, we found a relatively large and significant modulation by the MJO and ER waves, a small yet significant modulation by Kelvin waves, and a modulation by MRG waves that failed our test of statistical significance.

For the MJO, the daily percentage genesis rate for the region is 2.6 times greater in the most conducive category compared to the least conducive category (Table 1). Comparing this to previous work, Hall et al. (2001) found a modulation of about 4:1 to the northwest of Australia, and 3:1 to the northeast, by their similarly defined MJO (see their Table 1). Thus it appears that the MJO's influence on TC genesis to the west of 100°E is somewhat less than that over the Australian region to the east. Considering that the amplitudes of the MJO signals in wind and convection are greater over near-Australian longitudes than farther west (Madden and Julian 1994; Wheeler and Hendon 2004), this result is, all else being equal, to be expected. Liebmann et al. (1994), on the other hand, found a modulation of only about 2:1 when defining just two

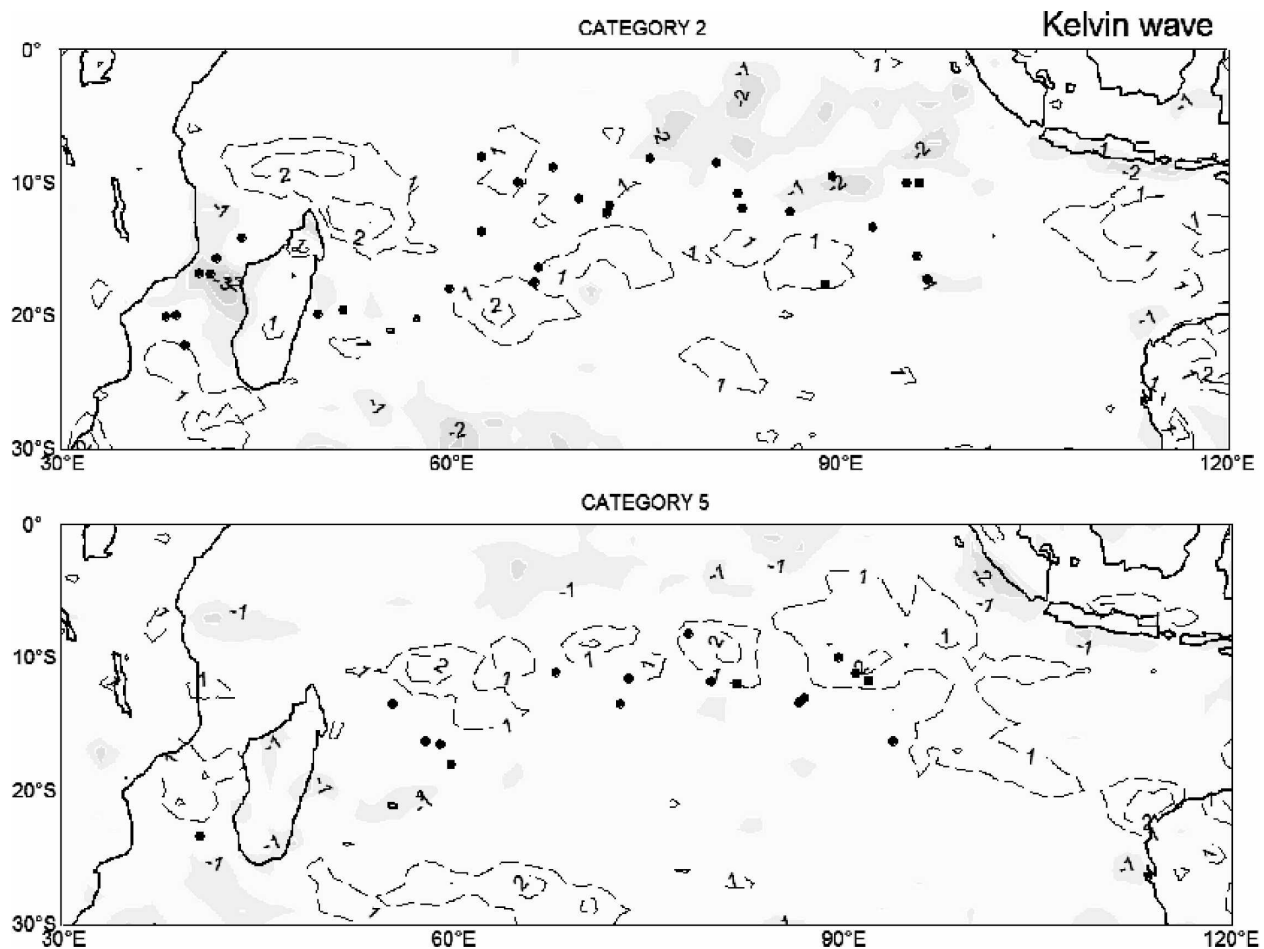


FIG. 17. As in Fig. 11, but for categories 2 and 5 of the Kelvin wave.

categories of the MJO (wet and dry), and accumulating TC statistics from locations across the whole Indian Ocean and western Pacific regions. Presumably, their definition of just two MJO categories acts to weaken the modulation signal.

Among the other waves, it is the modulation by the ER wave that is most pronounced. Indeed, the strength of its modulation was found to be as strong as that provided by the MJO, with a daily percentage genesis rate 2.7 times higher in its category 1 than category 4 (Table 1).

The attribution of the observed TC modulation was studied by looking at composites of fields of 850-hPa vorticity, vertical shear of the zonal wind between the 200- and 850-hPa levels, and OLR. The vorticity and shear fields form the basis of the previously identified dynamic conditions for TC development, while the OLR indicates the general presence of convective disturbances from which TCs can form. For the MJO, the observed TC modulation was best attributable to both

the vorticity and shear fields. For the ER wave, on the other hand, the modulation was most readily attributable to the OLR and vorticity fields. For the Kelvin and MRG waves, despite producing less pronounced or significant TC modulation, attribution could be made to the vorticity and OLR fields, respectively. Obviously, there appears to be no single factor to which subseasonal TC modulation can be attributed, an important result from this study.

We conclude that TC genesis over the south Indian Ocean does have a real and identifiable modulation signal caused by large-scale atmospheric wave variability, and at least for the MJO and ER waves, this signal is large enough to warrant exploitation for prediction purposes. Both these large-scale disturbances have previously been shown to have some predictability up to a few weeks or several days in advance, respectively (Waliser et al. 2003; Wheeler and Weickmann 2001); thus the time scales are quite relevant for extending the current TC predictability provided by numerical weather

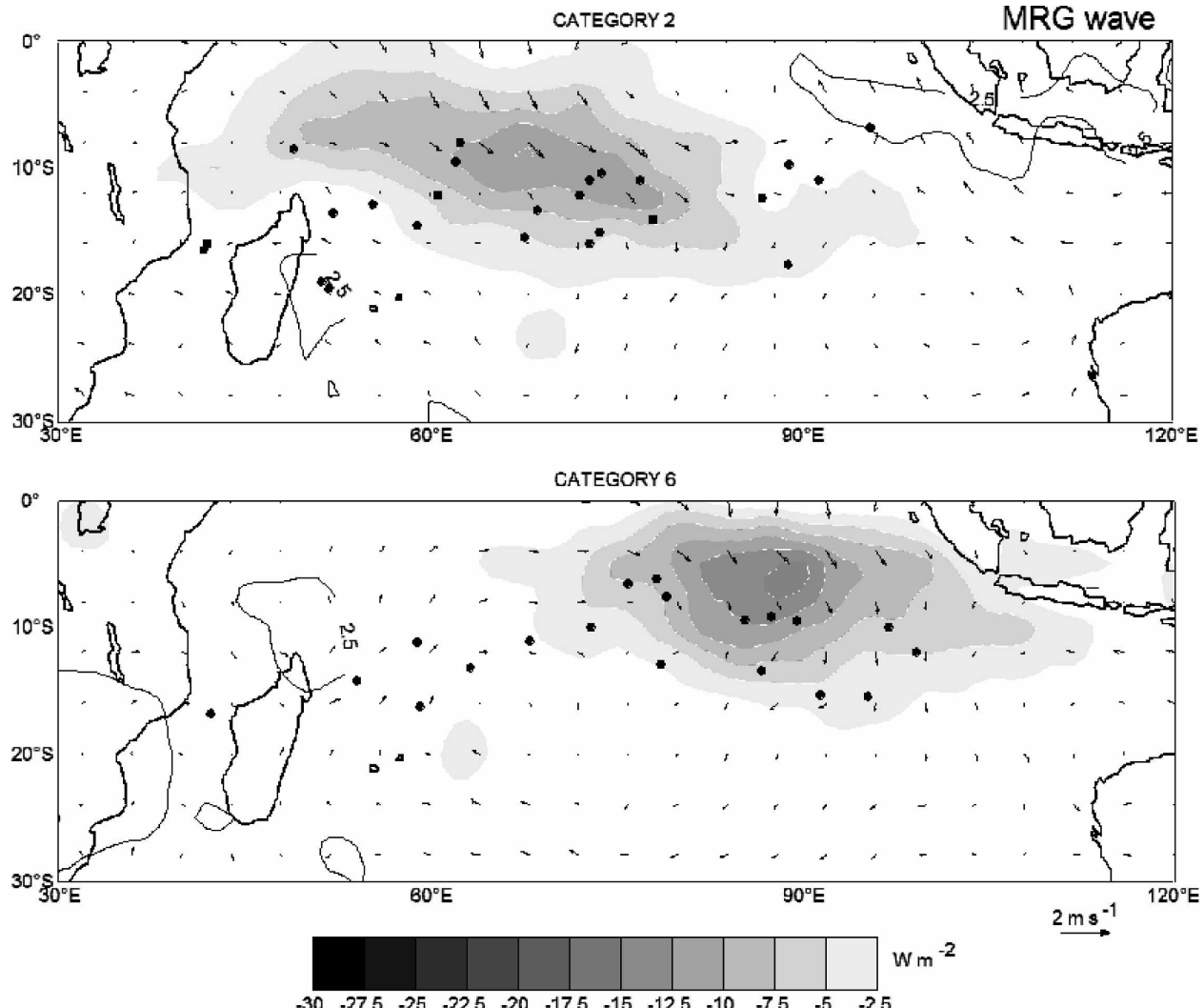


FIG. 18. As in Fig. 10, but for categories 2 and 6 of the MRG wave.

prediction techniques. The development of an empirical forecast model, incorporating the MJO and ER waves as predictors, is currently under way.

Acknowledgments. The first author would like to thank Météo-France (Cellule Recherche Cyclone) for providing the gridded ECMWF model analyses, the TC best-track database, and technical support. Interpolated OLR data were obtained from the NOAA-CIRES Climate Diagnostics Center, Boulder, Colorado, from their Web site <http://www.cdc.noaa.gov/>. Initial aspects of this work were completed while the first author was a visitor to the Bureau of Meteorology Research Centre in Melbourne, Australia. We thank Bertrand Timbal, John McBride, and two anonymous reviewers, whose suggestions helped improve the paper.

REFERENCES

- Arkin, P. A., and P. E. Ardanuy, 1989: Estimating climatic-scale precipitation from space: A review. *J. Climate*, **2**, 1229–1238.
- Dickinson, M., and J. Molinari, 2002: Mixed Rossby–gravity waves and western Pacific tropical cyclogenesis. Part I: Synoptic evolution. *J. Atmos. Sci.*, **59**, 2183–2196.
- Frank, W. M., 1987: Tropical cyclone formation. *A Global View of Tropical Cyclones*, R. L. Elsberry, Ed., Office of Naval Research, 53–90.
- Gray, W. M., 1968: Global view of the origin of tropical disturbances and storms. *Mon. Wea. Rev.*, **96**, 669–700.
- , 1979: Hurricanes: Their formation, structure, and likely role in the tropical circulation. *Meteorology over the Tropical Oceans*, D. B. Shaw, Ed., Royal Meteorological Society, 155–218.
- Hall, J., A. J. Matthews, and D. Karoly, 2001: The modulation of tropical cyclone activity in the Australian region by the Madden–Julian oscillation. *Mon. Wea. Rev.*, **129**, 2970–2982.

- Hartmann, D. L., M. L. Michelsen, and S. A. Klein, 1992: Seasonal variations of tropical intraseasonal oscillations: A 20–25-day oscillation in the western Pacific. *J. Atmos. Sci.*, **49**, 1277–1289.
- Hendon, H. H., and B. Liebmann, 1994: Organization of convection within the Madden–Julian oscillation. *J. Geophys. Res.*, **99**, 8073–8083.
- Kemball-Cook, S. R., and B. C. Weare, 2001: The onset of convection in the Madden–Julian oscillation. *J. Climate*, **14**, 780–793.
- Landsea, C. W., G. D. Bell, W. M. Gray, and S. B. Goldenberg, 1998: The extremely active 1995 Atlantic hurricane season: Environmental conditions and verification of seasonal forecasts. *Mon. Wea. Rev.*, **126**, 1174–1193.
- Liebmann, B., and C. Smith, 1996: Description of a complete (interpolated) outgoing longwave radiation dataset. *Bull. Amer. Meteor. Soc.*, **77**, 1275–1276.
- , H. H. Hendon, and J. D. Glick, 1994: The relationship between tropical cyclones of the western Pacific and Indian Oceans and the Madden–Julian oscillation. *J. Meteor. Soc. Japan*, **72**, 401–412.
- Lo, F., and H. H. Hendon, 2000: Empirical prediction of the MJO. *Mon. Wea. Rev.*, **128**, 2528–2543.
- Madden, R., and P. R. Julian, 1994: Observations of the 40–50-day tropical oscillation—A review. *Mon. Wea. Rev.*, **122**, 814–837.
- McBride, J. L., and R. Zehr, 1981: Observational analysis of tropical cyclone formation. Part II: Comparison of non-developing versus developing systems. *J. Atmos. Sci.*, **38**, 1132–1151.
- , and T. D. Keenan, 1982: Climatology of tropical cyclone genesis in the Australian region. *J. Climatol.*, **2**, 13–33.
- Maloney, E. D., and D. L. Hartmann, 2000a: Modulation of hurricane activity in the Gulf of Mexico by the Madden–Julian oscillation. *Science*, **287**, 2002–2004.
- , and —, 2000b: Modulation of eastern North Pacific hurricanes by the Madden–Julian oscillation. *J. Climate*, **13**, 1451–1460.
- Matthews, A. J., 2000: Propagation mechanisms for the Madden–Julian oscillation. *Quart. J. Roy. Meteor. Soc.*, **126**, 2637–2652.
- Merrill, R. T., 1988: Environmental influences on hurricane intensification. *J. Atmos. Sci.*, **45**, 1678–1687.
- Molinari, J., and D. Vollaro, 2000: Planetary- and synoptic-scale influences on eastern Pacific tropical cyclogenesis. *Mon. Wea. Rev.*, **128**, 3296–3307.
- , D. Knight, M. Dickinson, D. Vollaro, and S. Skubis, 1997: Potential vorticity, easterly waves, and eastern Pacific tropical cyclogenesis. *Mon. Wea. Rev.*, **125**, 2699–2708.
- Nakazawa, T., 1986: Intraseasonal variations of OLR in the tropics during the FGGE year. *J. Meteor. Soc. Japan*, **64**, 17–34.
- Slingo, J. M., D. P. Rowell, K. R. Sperber, and F. Nortley, 1999: On the predictability of the interannual behaviour of the Madden–Julian oscillation and its relationship with El Niño. *Quart. J. Roy. Meteor. Soc.*, **125**, 583–609.
- Sobel, A. H., and E. D. Maloney, 2000: Effect of ENSO and the MJO on western North Pacific tropical cyclones. *Geophys. Res. Lett.*, **27**, 1739–1742.
- Sperber, K. R., 2003: Propagation and the vertical structure of the Madden–Julian oscillation. *Mon. Wea. Rev.*, **131**, 3018–3037.
- Straub, K. H., and G. N. Kiladis, 2002: Observations of a convectively coupled Kelvin wave in the eastern Pacific ITCZ. *J. Atmos. Sci.*, **59**, 30–53.
- Waliser, D. E., K. M. Lau, W. Stern, and C. Jones, 2003: Potential predictability of the Madden–Julian oscillation. *Bull. Amer. Meteor. Soc.*, **84**, 33–50.
- Wheeler, M., and G. N. Kiladis, 1999: Convectively coupled equatorial waves: Analysis of clouds and temperature in the wave-number–frequency domain. *J. Atmos. Sci.*, **56**, 333–358.
- , and K. M. Weickmann, 2001: Real-time monitoring and prediction of modes of coherent synoptic to intraseasonal tropical variability. *Mon. Wea. Rev.*, **129**, 2677–2694.
- , and H. H. Hendon, 2004: An all-season real-time multivariate MJO index: Development of an index for monitoring and prediction. *Mon. Wea. Rev.*, **132**, 1917–1932.
- , and J. L. McBride, 2005: Australian–Indonesian monsoon. *Intraseasonal Variability in the Atmosphere–Ocean Climate System*, W. K. M. Lau and D. E. Waliser, Eds., Praxis, 125–173.
- , G. N. Kiladis, and P. J. Webster, 2000: Large-scale dynamical fields associated with convectively coupled equatorial waves. *J. Atmos. Sci.*, **57**, 613–640.
- WMO, 2002: Tropical cyclone operational plan for the south-west Indian Ocean. Rep. TCP-12, TD No. 577, 59 pp.
- Wong, M. L., and J. C. L. Chan, 2004: Tropical cyclone intensity in vertical wind shear. *J. Atmos. Sci.*, **61**, 1859–1876.